ORIGINAL PAPER

Beyond the beak: Brain size and allometry in avian craniofacial evolution

Jesús Marugán-Lobón[1,2] | Sergio M. Nebreda[1] | Guillermo Navalón[1,3] | Roger B. J. Benson[4]

[1]Unidad de Paleontología, Dpto. Biología, Universidad Autónoma de Madrid, Madrid, Spain

[2]Dinosaur Institute, Natural History Museum of Los Angeles County, Los Angeles, California, USA

[3]Department of Earth Sciences, University of Cambridge, Cambridge, UK

[4]Department of Earth Sciences, University of Oxford, Oxford, UK

Correspondence
Jesús Marugán-Lobón, Unidad de Paleontología, Dpto. Biología, Universidad Autónoma de Madrid, 28049, Madrid, Spain.
Email: jesus.marugan@uam.es

Abstract

Birds exhibit an enormous variety of beak shapes. Such remarkable variation, however, has distracted research from other important aspects of their skull evolution, the nature of which has been little explored. Key aspects of avian skull variation appear to be qualitatively similar to those of mammals, encompassing variation in the degree of cranial vaulting, cranial base flexure, and the proportions and orientations of the occipital and facial regions. The evolution of these traits has been studied intensively in mammals under the Spatial Packing Hypothesis (SPH), an architectural constraint so-called because the general anatomical organization and development of such skull parts makes them evolve predictably in response to changes in relative brain size. Such SPH predictions account for the different appearances of skull configurations across species, either in having longer or shorter faces, and caudally or ventrally oriented occiputs, respectively. This pattern has been morphometrically and experimentally proven in mammals but has not been examined in birds or other tetrapods, and so its generality remains unknown. We explored the SPH in an interspecific sample of birds using three-dimensional geometric morphometrics. Our results show that the dominant trend of evolutionary variation in the skull of crown-group birds can be predicted by the SPH, involving concomitant changes in the face, the cranial vault and the basicranium, and with striking similarities to craniofacial variation among mammals. Although craniofacial variation is significantly affected by allometry, these allometric effects are independent of the influence of the SPH on skull morphology, as are any effects of volumetric encephalization. Our results, therefore, validate the hypothesis that a general architectural constraint underlies skull homoplasy evolution of cranial morphology among avian clades, and possibly between birds and mammals, but they downplay encephalization and allometry as the only factors involved.

KEYWORDS
avian, brain, constraint, cranial base, craniofacial, geometric morphometrics

1 | INTRODUCTION

The avian beak exhibits tremendous evolutionary variation and has been a target of ecomorphological and evolutionary studies (Abzhanov et al., 2006; Bhullar et al., 2015; Friedman et al., 2019; Herrel et al., 2005; Mallarino et al., 2012; Navalón et al., 2019). Despite its striking diversity of shapes and sizes (Bright et al., 2016; Felice et al., 2019; Navalón et al., 2019; Zusi, 1993), the osteological component of the beak is largely constituted by a single bone, the premaxilla (Bhullar et al., 2015), situated at the most anterior portion of the facial skeleton. The facial skeleton is, in turn, parceled into several parts which are built by individual bones including the jugals, maxillae, nasals, lachrymals, and ethmoids (Zusi, 1993). Differences in the organization of these bones result in large variation in facial morphology across clades (Figure 1). For instance, the beak of the woodcock (*Scolopax rusticola*) is long and straight, and the face is downwardly oriented, such that the skull appears bent, or angled. In contrast, many other birds, (e.g. snakebirds – *Anhinga*, and albatrosses – *Diomedea*; Figure 1) also have a long and straight beak, but the facial skeleton is oriented in line with the main axis of the cranium, giving the skull a more elongated appearance. Importantly, such facial differences among bird skulls occur concomitantly with changes in the doming of the cranial vault and the orientation of the rear of the skull, the occiput, which connects the head to the neck. The occiput is also built by several bones and is oriented ventrally in many birds, including extreme cases such as in woodcocks or hummingbirds. In contrast, the occiput is notably caudally facing in many birds, including some aquatic birds like swans, cormorants, snakebirds, and many other waterbirds (Figure 1) but also in some terrestrial forms such as galliforms and arboreal forms such as macaws. There is also evidence that such cranio-facial differences among birds involve changes in the anatomy of the endocranium (Duijm, 1951; Lang, 1956; Iwaniuk & Nelson, 2002; Marugán-Lobón & Buscalioni, 2009), suggesting a correlation to brain evolution that has never been tested.

Descriptions of such variation in avian skull organization so far are either cursory in nature (Zusi, 1993) and/or were traditionally focused on the adaptations of exemplar species to specific ecologies (Marinelli, 1929; Hofer, 1952; Lang, 1956; Duijm, 1951; Werner, 1962). Therefore, it remains unknown why such features of skull variation evolved convergently across many lineages and are therefore ubiquitous among Neornithes (Klingenberg & Marugán-Lobón, 2013). This contrasts with the rich history of the study of craniofacial evolution in mammals, which has been subject to decades-long
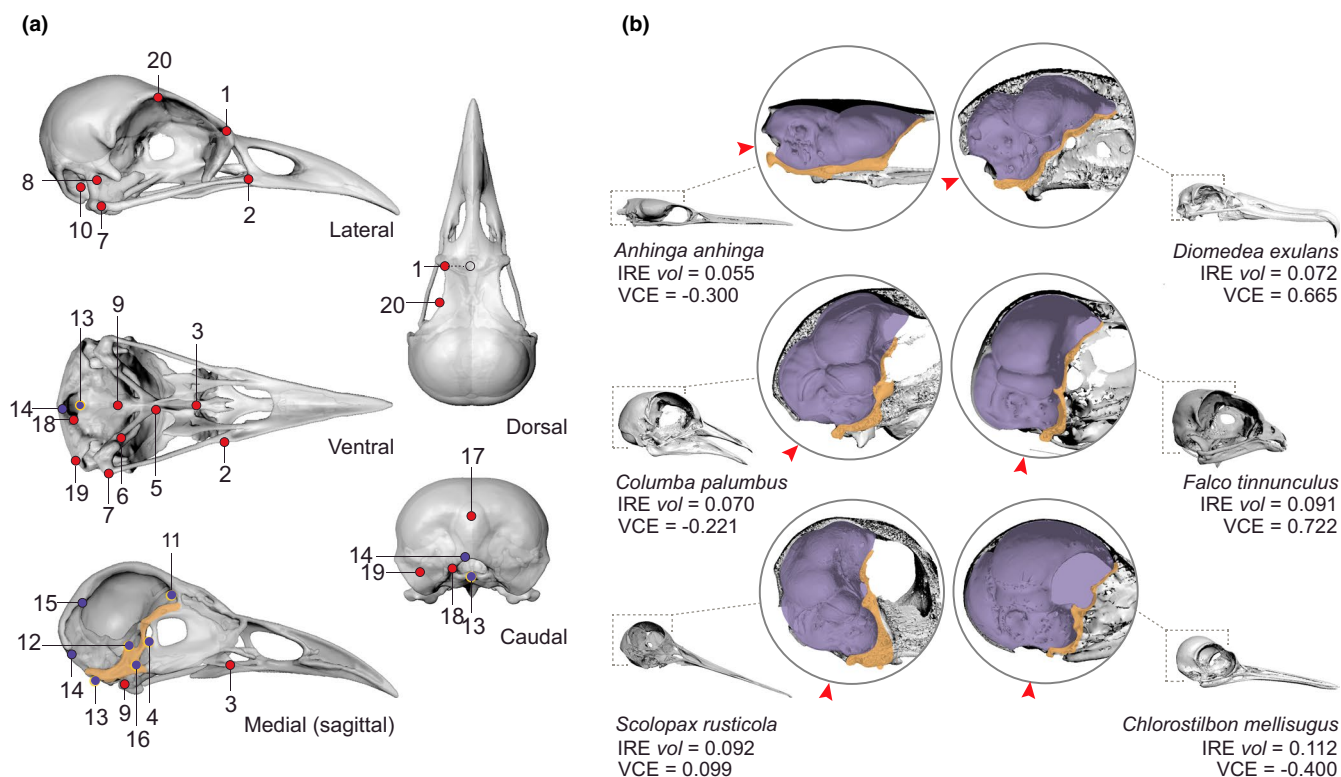

FIGURE 1 The avian skull. (a) Example of an avian skull (digital render of a Crow skull) in different anatomical views along with the landmark configuration utilized in this study. Midline plane landmarks from the endocranium are in blue and basicranial landmarks are highlighted in yellow Description of the anatomical correspondence of each landmark is listed in the SI (Table S2). (b) Midline section of the skulls of selected avian taxa showing their differences in endocranial anatomy; numbers are their values of IRE *vol* and VCE. Insets are close-ups of each of the skull endocrania, which are shown deliberately confronted to visually show the notable differences in brain (denoted by its endocast, shown in blue) and cranial base (shown in yellow) orientations and shapes. The red arrows indicate the position of the foramen magnum

multidisciplinary research, often motivated by an interest in hominin evolution.

The main trends of craniofacial variation across mammals, which are remarkably similar to those of birds (Hofer, 1952), are often characterized using a relatively simple model, which mainly invokes the product of restricted epigenetic pathways connected with brain growth (Hallgrimsson et al., 2007). This conceptual model, the "Spatial Packing Hypothesis" (SPH), posits that the growth of the brain causes changes in the topology of its bony base inside the cranium which has cascading and predictable effects on the shape of the whole skull (Bastir et al., 2010; Dubrul & Lasskin, 1961; Enlow & Hans, 1996; Gould, 1975, 1977; Lieberman et al., 2000a, 2000b; McCarthy, 2001; Ross et al., 2004; Ross & Ravosa, 1993; Strait, 1999). At its core, the SPH model describes coordinated evolution of the face and the basicranial midline (Bastir & Rosas, 2009), entailing that morphological integration—the correlated evolution of traits (Olson & Miller, 1958)—has a prime role in shaping the phenotypic diversity of the skull. This is valuable because the concept of integration provides a conceptual and multidisciplinary scaffold relatively apart from functional rationales, from which to link morphological evolution with genetics, development, and phylogeny into a unified agenda (Goswami et al., 2014).

Under the SPH model, the main features of the primate skull, including its domed cranial vault, highly flexed cranial base, and retracted facial skeleton, are explained mostly as an epiphenomenon triggered by evolutionary increases in relative brain size (encephalization) (Bastir & Rosas, 2009). In its simplest version, this model explains that by growing at faster rates than its physical skeletal envelope, the brain occupies much more space, forcing the cranial base to bend concavely, hence doming the vault, and ventrally reorienting the occiput (and the foramen magnum), causing the face to reorient and shorten (Lieberman, 2011; Lieberman et al., 2008; Lieberman et al., 2000a, 2000b). In its most encompassing version, the SPH entails that brain development and its interaction with skeletal growth—particularly of the cranial base—triggers a myriad of complex tissue and molecular signaling cues that shape the whole skull organization from very early in ontogeny. This complex network of pathways is far from being completely understood (Lesciotto & Richstmeier, 2019). Nevertheless, it evidences that the role of developmental architecture in the production of phenotypic variation is central to understanding the evolutionary diversification of organismal morphology (Parsons et al., 2011).

Bird skulls are highly morphologically integrated (Bright et al., 2016; Navalón et al., 2020), entailing that their evolutionary variation is constrained along particular axes of change (Villmoare, 2012). The logic of "evolutionary constraint" underlies the likelihood of homoplasy (Wake et al., 2011), and could explain the observed high frequency of craniofacial homoplasy across avian phylogeny (Klingenberg & Marugán-Lobón, 2013). Birds are also among the most encephalized vertebrates (Ksepka et al., 2020), and some birds, such as passerines and raptors, display a suite of traits that are comparable to those of primates, namely, domed cranial vaults, concavely flexed cranial bases, and retracted facial skeletons. Given

the evolutionary importance of encephalization across vertebrates (Striedter, 2005), and that the tight coupling of brain and skull morphology is invariant and highly constrained (Young et al., 2014; Fabbri et al., 2017; Parsons et al., 2011), it is possible that the developmental pathways that structure skull evolution in mammals and birds are comparable. To address this hypothesis, here we examined the evolutionary history of skull variation across avian phylogeny using 3D statistical shape Analysis (Geometric Morphometrics) combined with phylogenetic comparative methods to test whether the SPH might explain the main features of avian skull variation across phylogeny.

2 | METHODS

Our sample includes the tridimensional volumes of the main outer and inner surfaces of the skull from 76 species of modern birds, encompassing 53 families and 28 avian orders (Table S1). Although the sample is small relative to described avian diversity, it spans a wide range of the avian phylogeny (Hackett et al., 2008, Jarvis et al., 2014, Prum et al., 2015), adequately characterizing the structural disparity of modern bird skulls across most of their ecological disparity (see e.g., Klingenberg & Marugán-Lobón, 2013). Fifty-two of the skulls belong to the Hess Collection housed at the Department of Ornithologie, Museum für Naturkunde in Berlin (for the preparation of the skulls, see Hesse, 1907 and Table S1). The skulls in this collection are conserved medially opened, enabling the registration of endo and exo-cranial geometric information out of a single side of the skull in each specimen (Figure 1). The remaining 24 skulls came from various other collections and were obtained via online virtual databases of μCT scanned specimens (www.morphosource.org) and by μCT scanning of museum specimens by RBJB (e.g., Bjarnason & Benson, 2021). Three-dimensional volumes were extracted from these μCT datasets using Avizo 9 (https://www.fei.com/softw are/amira-avizo/) (see Table S1). A tridimensional configuration of 20 landmarks (LMs; Table S2) was digitized (with a Microscribe G2 [Immersion Corp.]) on the skulls from the Hess Collection and using Stratovan Checkpoint (v. 2019.03.04.1102) on the skulls derived from μCT data. Only one side of the skull was digitized, the choice of side was determined only either by availability or preservation, and the obtained landmark coordinates were symmetrically reflected to match the opposite side of the skull and stitched to its counterpart using the midline landmarks with the software FileConverter (http://www.flywings.org.uk/fileConverter_page.htm), making a total set of 35 LMs (five of them placed on the skull midline; Figure 1a and Table S2) to build a full 3D coordinates configuration. The whole LM configuration homogeneously captures features of the facial skeleton and the neurocranium, as well as endocranial features of the midline of the neurocranium, including the cranial base and the cranio-cervical junction (e.g., the foramen magnum). The anatomical description of our landmarks follows Baumel and Witmer (1993) and Couly et al. (1993) (Table S2). We did not digitize the shape of the beak, because its notable length in many species misrepresents the real size of the

skull (Brooke et al., 1999), and it exhibits large inter-specific variation and inevitably overprints variation among and within other regions of the face and cranium, whose structural evolutionary variability is the focus of this study. Furthermore, large and localized variation in beak morphology can demonstrably lead to an improper alignment of more posterior cranial structures during Procrustes superposition (e.g., Pinocchio effects derived from the Least Squares step of the Generalized Procrustes Superimposition; Klingenberg & Marugán-Lobón, 2013; Kulemeyer et al., 2009; Marugán-Lobón & Buscalioni, 2004).

We use phylogenetic comparative methods, which account for the phylogenetic non-independence of species traits (Felsenstein, 1985). The phylogenetic framework for these analyses was generated using a maximum clade credibility (MCC) time-calibrated supertree of the 76 species using TreeAnnotator (Rambaut & Drummond, 2014) derived from a population of 10,000-stage 2 species trees based on a Hackett (2008) backbone (see www.birdtree.org and Jetz et al., 2012 for full details on the nature of these source trees). Branch lengths were set equal to "Common ancestor" node heights.

The full bilaterally symmetrical 3D landmark configurations were superimposed using the Generalized Least Squares Procrustes criterion (Rohlf & Slice, 1990) to extract size (skull centroid size) and shape (Procrustes coordinates) variables. To visualize the major aspects of craniofacial variation among birds, we conducted Principal Components Analysis (PCA) of the Procrustes coordinates. We explicitly displayed the evolutionary history of shape variation by including the reconstruction of ancestral shapes of all the nodes in the time-calibrated MCC phylogeny using maximum likelihood (Maddison, 1991; Rohlf, 2002). We visualized this mapping by plotting the ancestral and descendent shapes over the PCA scatterplots (i.e., as a "phylomorphospace").

To describe size and encephalization we calculated three different geometric variables for each of the skulls: skull centroid size (SCS), and two different indexes of relative encephalization (IRE; Strait, 1999) plus a volumetric coefficient of encephalization (VCE; Sayol et al., 2018). SCS is calculated as the square root of the sum of the squared distances of each landmark to the centroid's landmarks configuration (Bookstein, 1991). IRE is a ratio that describes the relationship between the size of the brain (numerator) to the total chord length of the cranial base (the mid-sagittal contour of the intracranial surface of the cranial base, the denominator; Strait, 1999). This index has been calculated in many ways in literature, yet it always renders nearly equivalent results. Here, its calculation was accommodated to the characteristic morphology of the avian skull and the available landmark data. We calculated this index in two different ways: (1) following the anthropological literature (e.g., Strait, 1999) using volumetric data (IRE *vol*), we used the cube root (to comply to dimensions of linear skull centroid size) of the brain volume (sourced from Sayol et al., 2018, see Table S1). List of specimens and data, divided by the centroid size of the midline of the cranial base from the foramen olfactorium (N. I), passing by the foramen opticum (N. II) and the sella to the occipital condyle (landmarks 11, 4, 12, and 13, respectively; see Figure 1a). Secondly, (2) an alternative IRE (IRE *mid*)

was calculated using the centroid size of the landmarks positioned along the midline of the brain (the midline plane of the endocranial cavity, landmarks 4, 11, 12, 13, 14, 15, and 16; Figure 1a), instead of the cube root of the brain volume, hence why it is labeled as IRE *mid*. Finally, the VCE of the 76 species was obtained from Sayol et al. (2018). These data estimations of relative brain size of each species were calculated as the residuals from a phylogenetic generalized least squares regression (PGLS) of absolute brain size against body mass, with both variables log_{10}-transformed prior to analysis.

All our univariate indexes were mapped as continuous traits on the phylogeny branches alone using maximum likelihood, and on phylogeny branches mapped over the principal axes of morphological variation (PC1-3), to visually compare their different distributions across the avian tree and their interaction with craniofacial shape, respectively. We did this using contMap and phylomorphospace functions of the R package phytools v.0.6–60 (Revell, 2012). Finally, we used the functions *phylosignal* and *phylosig* of the packages phytools (Revell, 2012) and geomorph, to quantify phylogenetic signal in our univariate and multivariate traits (i.e., the extent to which closely related species show similar values compared to those of more distantly related species). Phylogenetic signal is quantified using Blomberg's K (or K_{mult}) with predicted values of 1 for a Brownian Motion model of evolution (diffusive evolution in which lineages are not strongly attracted to certain trait values), values less than 1 indicating weaker phylogenetic signal, and values close to 1 or surpassing 1 indicate stronger phylogenetic signal.

We used PGLS Procrustes ANOVA (Collyer et al., 2015) to explore the relationship between skull shape variation, skull size, and encephalization using the R packages geomorph v.3.3.0 (Adams et al., 2020) and RRPP v.0.3.0 (Collyer & Adams, 2018). We initially inspected four PGLS multivariate linear regressions (Monteiro, 1999) on Procrustes coordinates as a function of the variables SCS, IRE *vol*, IRE *mid*, and VCE. The statistical significance for all PGLS multivariate regressions and pairwise comparisons was assessed using permutation tests of 10,000 iterations against a null hypothesis of independence. The sums of squares and cross-products were performed by the hierarchical type (type II) as independent variables are likely to covary with phylogeny (Adams & Collyer, 2018, Procrustes MANOVA).

We then constructed a set of multiple regression models using PGLS Procrustes ANOVA, to characterize the independent effects of skull size (SCS), skull base length (i.e., the centroid size of the landmarks conforming the midline of the cranial base from the foramen olfatorium (N. I), passing by the foramen opticum (N. II) and the sella to the occipital condyle), and brain size (3D endocranial centroid size) on skull shape. This was done by evaluating models that include combinations of those variables as follows: (i) skull shape ~skull size + brain size; (ii) skull shape ~skull size + skull base length; and (iii) skull shape ~skull size + brain size + skull base length. Skull size in these models was the log_{10} skull centroid size and brain size was the log_{10} 3D endocranial centroid size (i.e., that used in calculating IRE *vol*). The p-values and R^2 of skull base

length in the third model describe the extent to which relative brain size influences skull shape, and the extent to which relative skull base length provides additional, independent information on skull shape that is not already explained by relative brain size. It, therefore, provides a test of the hypothesis that major aspects of cranial variation in birds are independent of the occurrence of encephalization.

We used the thin-plate spline (Bookstein & Greene, 1993) to graphically display the shape changes along the different axes of variation (PCs, PGLS regression vectors), namely, as deviations from the mean shape warped on the tri-dimensional skull surface of the species most similar to the mean skull shape (*Corvus corone*) using the program Landmark (v. 3.0.0.6; IDAV).

3 | RESULTS

The indexes of relative encephalization (IRE *vol* & IRE *mid*) and the volumetric coefficient of encephalization (VCE) exhibit starkly different phylogenetic distributions; VCE shows a much higher phylogenetic signal ($K = 1.329$; Figure 2a, Table S3) indicating that closely related taxa are more similar than expected under diffusive evolution (Brownian Motion). Differences in the distributions of these variables are expected because the IRE variables compared brain size to skull measurements, whereas VCE compares brain size to body mass, and so contains a signal of head size relative to body size

that is not included in the IRE variables. Furthermore, the relationship between both our IRE variables and the VCE is not statistically significant, corroborating that the IRE and VCE express different aspects of encephalization in birds (Figure 2b). In contrast, and expectedly, IRE *mid* and IRE *vol* are highly correlated with skull shape variation ($r = 0.733$; $R^2 = 0.32$; $F = 34.59$; $Z = 2.15$; $Pr (>F) = 0.0001$; PGLS Procrustes ANOVA), despite each capturing different dimensions of endocranial variation (2D and 3D, respectively). However, the relatively low R^2 of this relationship suggests that variation in the IRE among birds cannot be captured entirely just by quantifying variation in the sagittal cross-section size of the brain (i.e., that mediolateral expansion of brain size make an important independent contribution to brain size).

The first three dimensions of the PCA explain slightly more than 50% of the cumulative variance of morphological change (Figures 3 and 4). The first principal component axis (PC1; 27% of explained variance), accounts for craniofacial shape differences that are identical to those previously reported in both qualitative (Lang, 1956; Marinelli, 1929) and in 2D quantitative traditional surveys (Duijm, 1951; Hofer, 1952), and using 2D shape analysis (Klingenberg & Marugán-Lobón, 2013; Marugán-Lobón & Buscalioni, 2004, 2006; Figure 4). Namely, positive PC1 scores are associated with more elongate skulls with a horizontally oriented craniocervical articulation (the foramen magnum opens caudally), while negative PC1 scores correspond with a caudoventrally-oriented craniocervical articulation (the foramen magnum opens ventrally), making the skull look
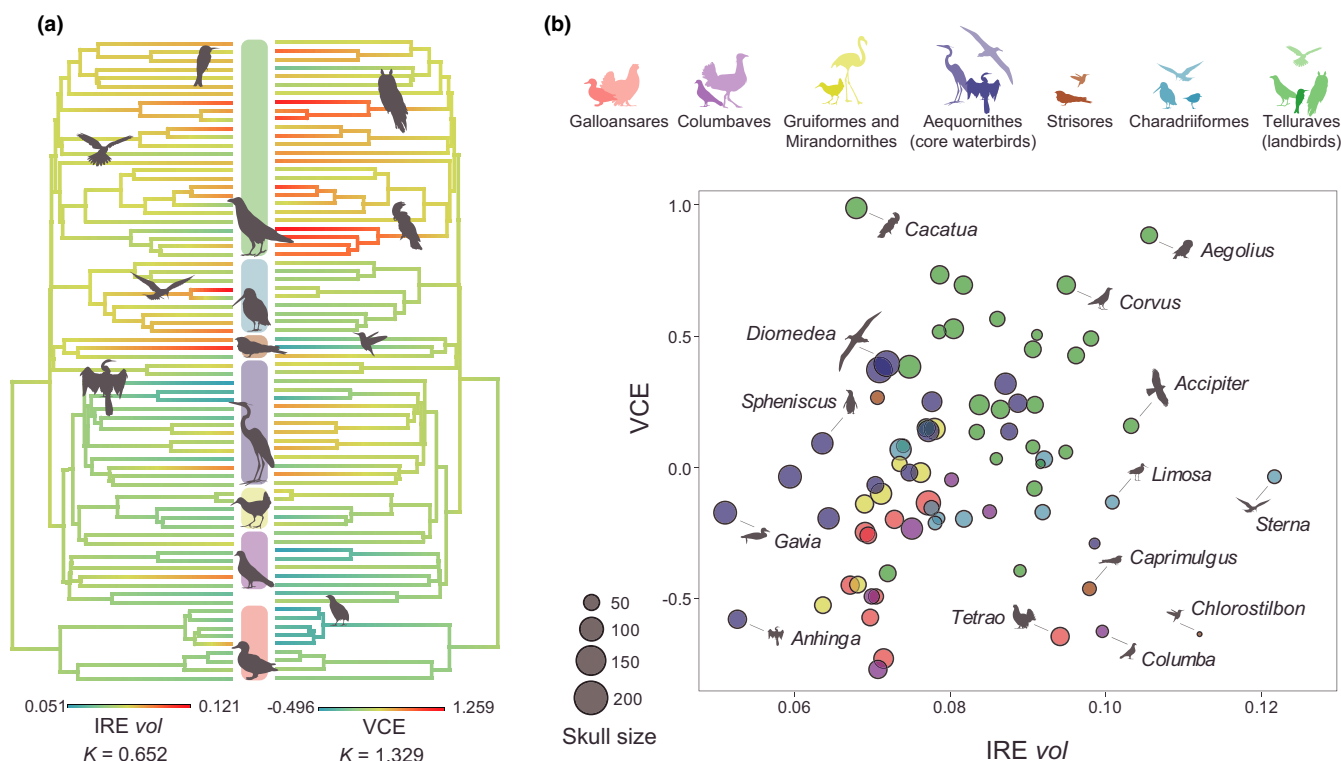

FIGURE 2 Avian phylogeny and the statistical relationship between the encephalization indexes. (a) Continuous mapping of IRE *vol* and VCE on the avian phylogeny used in the present study to show their different distribution (i.e., their different phylogenetic distribution). (b) PGLS regression Bubble-plot. The scatter is between IRE *vol* and VCE, and skull size (centroid size) is plotted as point size for each species
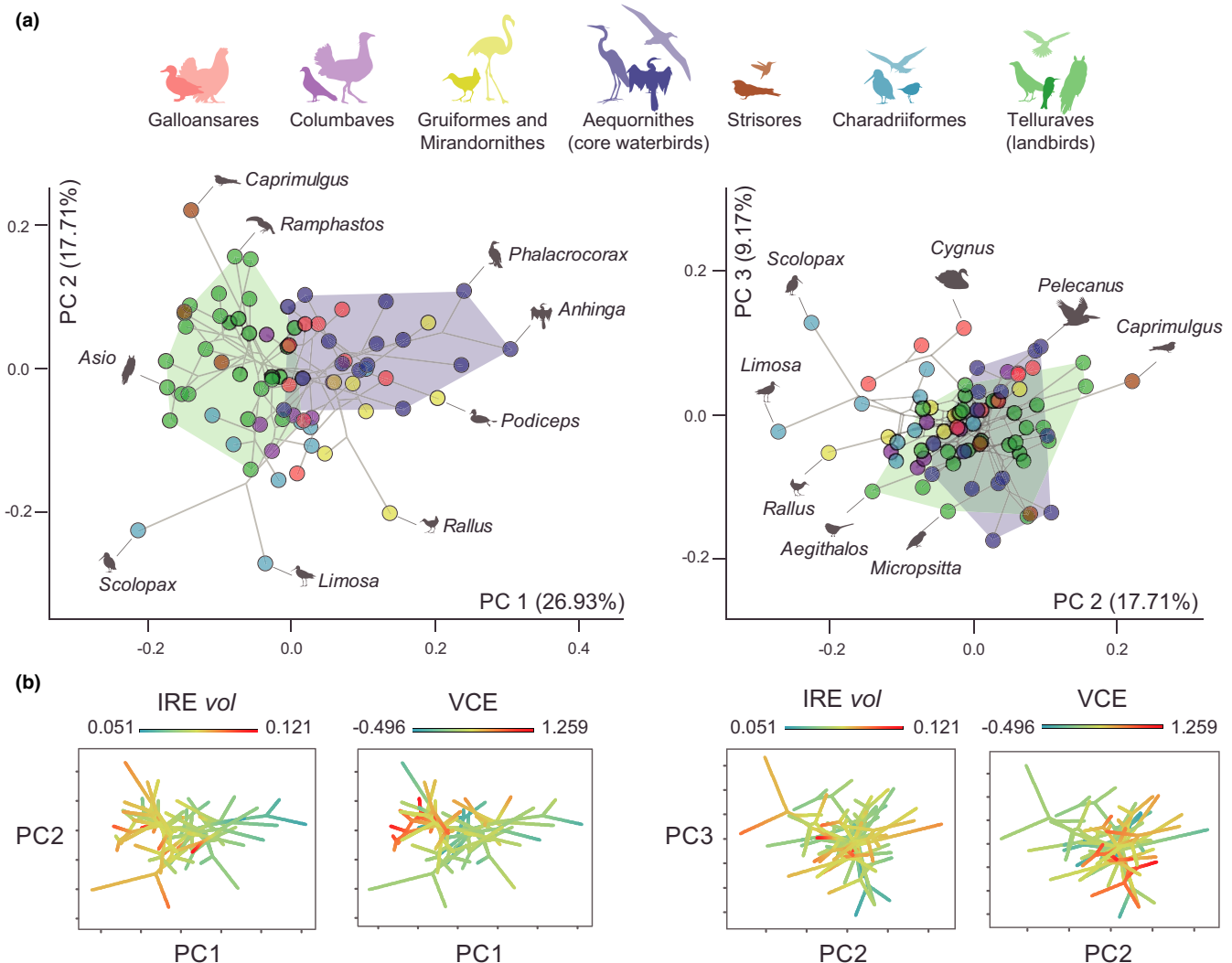
(a)

(b)

FIGURE 3 Craniofacial variation of the avian skull. (a) Phylomorphospaces show the first three axes of shape variation as accounted by PCA. Notice the divergence between "core landbirds" and "core waterbirds" along the PC1 axis. (b) Mapping of IRE *vol* and VCE across phylomorphospace

as if it was bent, with a ventrally inclined facial skeleton (Figure 4). Notably, the cranial base is shorter and ventrally more concave in species with more negative PC1 scores. The whole skull of these species is also relatively wider, while possessing relatively rostrocaudally reduced faces, a previously unappreciated feature of avian craniofacial variation (Figure 4). PC2 explains 18% of the variance and mainly accounts for variation in the coronal plane, mostly accounting for the width of the whole skull. Finally, PC3 encompasses about 9% of shape variance and largely accounts for the relative expansion or contraction of the face, its angle with respect to the neurocranium and changes in the relative width of the cranial base (including quadrates and pterygoids).

The clearest phylogenetic pattern in the PCA plot is the deep shape divergence among two main clades, the "core waterbirds" or Aequornithes and "core landbirds," or Telluraves, mainly unfolding along PC1 (Figure 3a). This dimension shows a strong phylogenetic signal, indicating that more recent divergences in this axis are characterized by proportionally greater similarity than

would be expected based on a Brownian Motion model of evolution ($K = 1.305$; Figure 3a,b, Table S3). The "core waterbirds" (storks, pelicans, tubenoses, penguins, boobies, and allies) are distributed along the positive scores of PC1, showing elongated and retroflexed skulls, with a caudally-oriented occiput. The cormorant (*Phalacrocorax carbo*) and the snakebird (*Anhinga anhinga*) are extreme representatives of these elongated skull-type morphologies. Similar PC1 scores are shown by many members of the Gruiformes (rails, cranes and kin) and the Mirandornithes (flamingos and grebes), while members of the Galloanserae (fowl and waterfowl) are largely associated with average scores in this axis. On the opposite extreme of PC1, "core landbirds" (encompassing eagles and vultures, owls, woodpeckers, kingfishers and allies, parrots, falcons, and passerines) are distributed along the negative scores of the PC1. These skulls are flexed, with shortened facial portions, wider neurocrania, and ventrally oriented occiputs. The most extreme representatives of this morphology among landbirds are owls. Landbirds share this region mostly with Charadriiformes
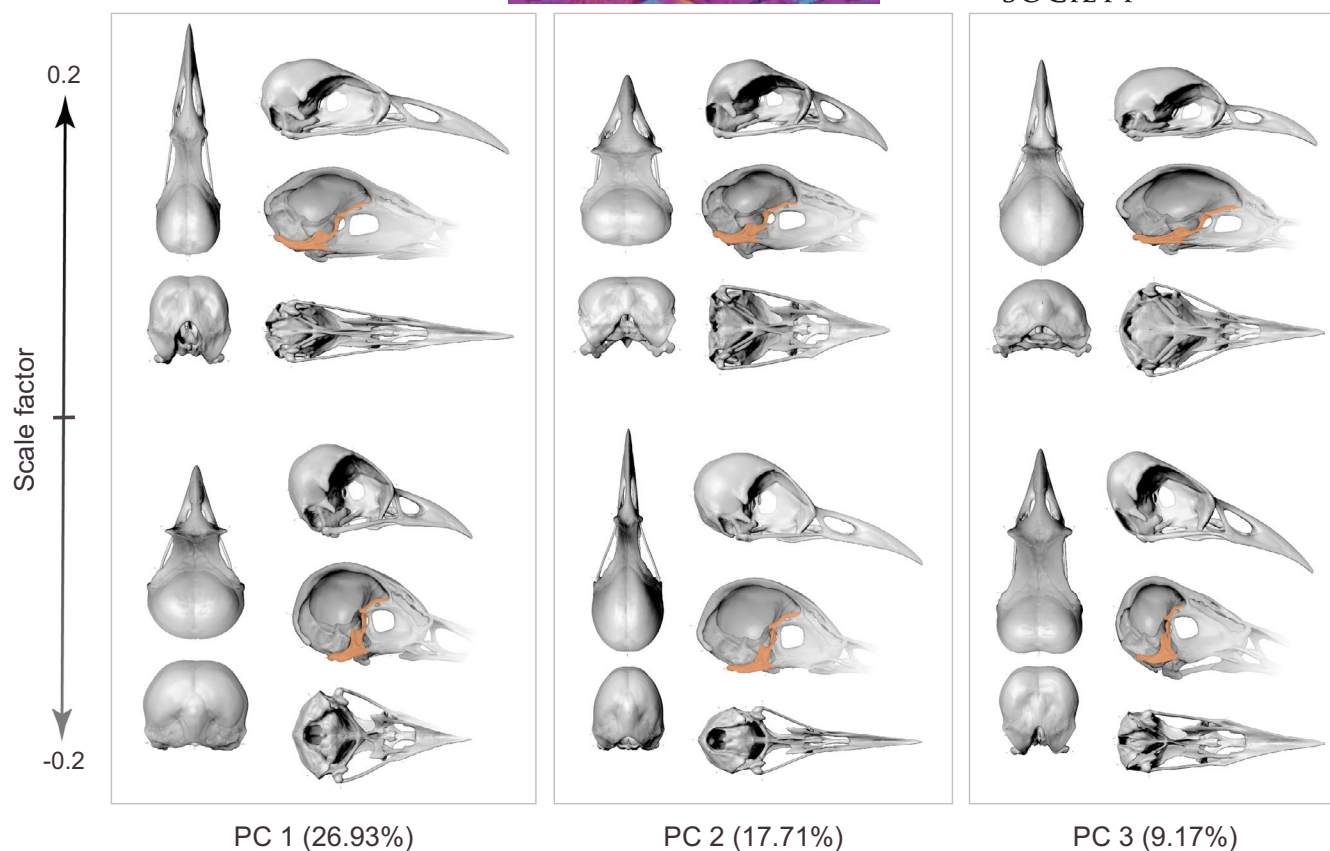
FIGURE 4 Main shape differences across avian skulls as accounted by the first three principal components of the PCA (see Figure 3). Skulls are shown in dorsal, lateral, ventral, caudal, and midline view (middle one, between lateral and ventral views). Scale factor of PC scores was set at ±0.2

(in particular, the woodcock – *Scolopax rusticola* – displays the most negative PC1 value of all birds) and Strisores (nightbirds, hummingbirds, and swifts), and partially with Columbaves (doves, sandgrouse, and mesites), distributing along more intermediate scores of this axis. PC2 differentiates less clearly core waterbirds and landbirds from the Gruiformes and the Charadriiformes, respectively, the latter showing narrower skulls.

IRE *vol* values distribute roughly as a gradient along the PC1 with lower values corresponding to elongate type skulls (positive PC1 scores) and higher values corresponding to flexed or bent type crania (negative PC1 scores; Figure 3b). In fact, results from the PGLS regressions between shape and both IREs show a significant and strong, nearly identical correlation (IRE *vol*: $R^2 = 0.059$; $F = 4.651$; $Z = 4.051$; $Pr\ (>F) = 0.0001$, and IRE *mid*: $R^2 = 0.053$; $F = 4.179$; $Z = 3.886$; $Pr\ (>F) = 0.0001$; Figure 6a and Table S4). Moreover, this distribution mirrors again the shape divergence between waterbirds and landbirds (see blue-to-green branches and red-to-yellow branches distribution in the phylomorphospace in Figure 3b). The vector of skull shape changes with increasing IRE correlates strongly with PC1 ($r = 0.933$). Thus, variation in IRE values is associated with a trend of shape change that is nearly identical to PC1 (Figures 6b and 4, respectively), and not PC2, which encompasses lateral variation. Moreover, taxa are clustered showing clade-specific morphologies and IRE values ($K = 1.143$; SI. Table

S3). In contrast, VCE values are more scattered across the phylomorphospace, suggesting a weaker relationship with skull shape and phylogeny (confirmed by results from the PGLS regression between shape and VCE: $R^2 = 0.02$; $F = 1.76$; $Z = 1.67$; $Pr\ (>F) = 0.049$; Table S4).

PGLS regression of skull shape against log-transformed skull centroid size (Figure 5) indicates that approximately 11% of craniofacial shape variance for all birds is allometric ($p < 0.001$) (Table S5). Allometric shape variation seems similar among most of the avian clades and is partially shared with shape variation along PC1, with larger skulls having proportionally larger faces, a clade-wide allometric trend that has also been identified for craniofacial evolution (Common Cranial Evolutionary Allometry, CREA) in mammals and other vertebrates (Werner, 1962; Marugán-Lobón & Buscalioni, 2009; Bright et al., 2016; in mammals: Cardini & Polly, 2013; Cardini, 2019; and Tamagnini et al., 2017; in Galliformes: Linde-Medina, 2016), whereas smaller skulls tend to be shorter and more flexed (Figure 5).

Although the skull shape differences accounted for by allometry (i.e., by skull shape ~skull size; Figure 5) are somewhat similar to those predicted by the regression using both IRE variables (Figure 6), and to that of the PC1 (Figure 4), none of them are strongly correlated ($r = 0.078$, and $r = 0.193$ respectively), implying some independence. Furthermore, a subsequent PGLS regression of shape residuals from
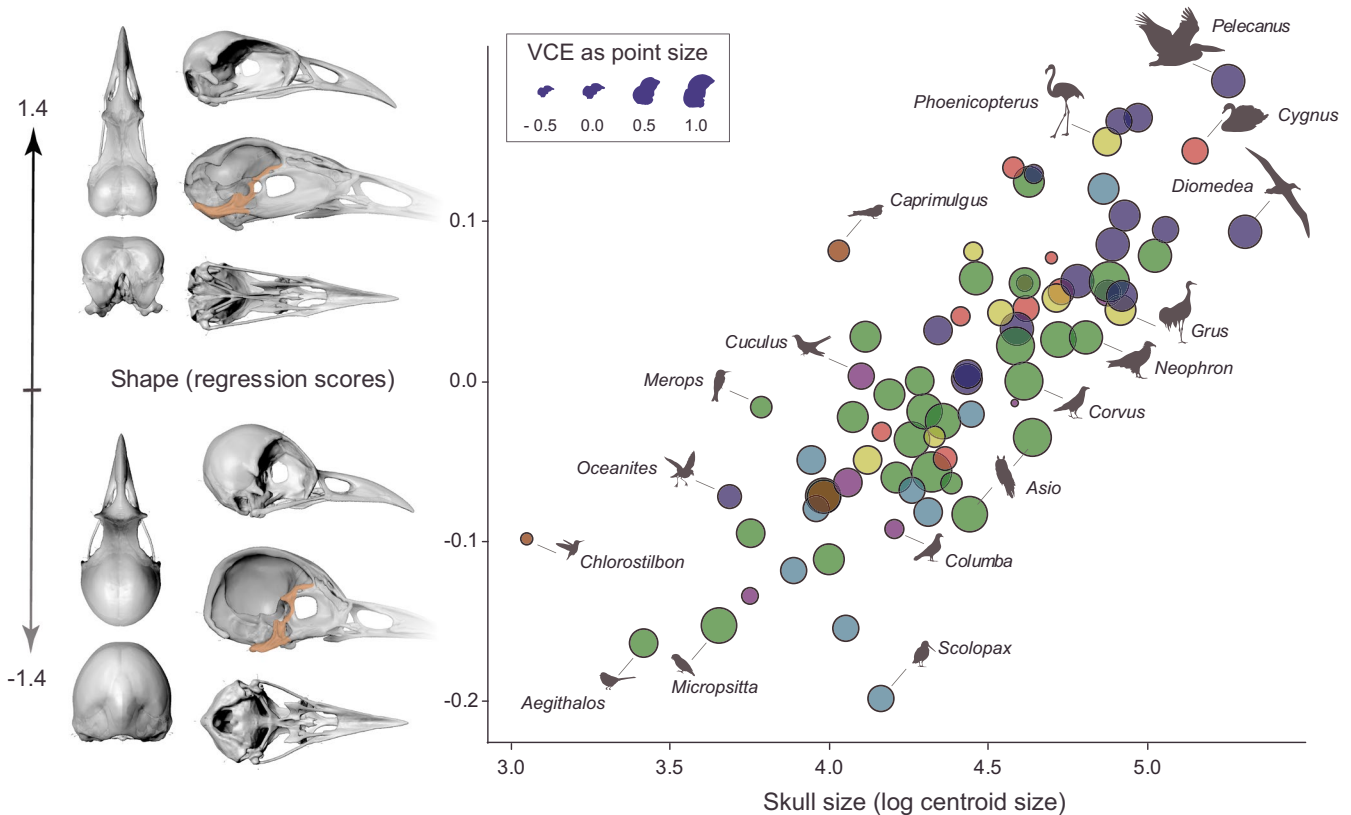
FIGURE 5 Evolutionary allometry of the avian skull. The Bubble-plot shows the scatter of log-centroid size of the skull (*x*-axis) predicting the shape vector that best correlates with size across shape space (*y*-axis). The skull shape changes predicted by size (evolutionary allometry) are shown on the left side of the plot, along the, and corresponding to the *y*-axis. Scale factor for the scores of such shape changes was set at ±1.4. Point size along the scatter is VCE for each

IRE *vol* on SCS yields an allometric vector (7% explained variance, $F = 5.6522$, $Z = 4.7766$, $Pr\,(>F) \leq 0.001$; Figures 6 and 7) that accounts for shape variation comparable to that of the previous allometric one (larger sizes associated with relatively larger faces and relatively smaller brains and vice versa for smaller sizes). However, clades seemingly overlap more along this new axis of allometric shape variation which is further confirmed by the phylogenetic signal decreasing when the IRE is factored out (from 1.143 to 0.690; Table S3). This stresses that craniofacial flexion in birds is laden with an important phylogenetic signal, while allometry seems to be a more pervasive phenomenon in craniofacial evolution in birds.

Our multiple regression models indicate that skull size and brain size provide independent information on skull shape, confirming the existence of an effect of relative brain size on skull shape (SI. Table S5; skull shape ~skull size + brain size). When skull base length is added to this model it is also statistically significant and explains a slightly greater amount of variation in skull shape ($R^2_{\text{skull base length}} = 0.63$; skull shape ~skull size + brain size + skull base length). The explanatory power of brain size is conserved within this model ($R^2 = 0.62$ compared to 0.67 when also including skull base length; Table S5), demonstrating that evolutionary shortening of the cranial base relative to overall skull size, and concomitant changes such as ventralization of the occiput, are independent of encephalization in birds.

4 | DISCUSSION

Bird skulls are highly morphologically integrated (Klingenberg & Marugán-Lobón, 2013) and some birds display cranial traits that are comparable to those of primates (domed cranial vault, flexed cranial base, and retracted facial skeleton). These observations hinted that tight coupling between brain morphology and skull morphology in birds could yield similar trends of skull variation than those seen in mammals. Our results reveal a significant correlation between the main patterns of skull shape variation and the indexes of relative encephalization (IRE *vol* and IRE *mid*) across avian phylogeny. Scaling differences between brain and cranial base sizes in birds are correlated with integrated morphological differences across the whole skull, including facial skeleton proportion, midline cranial base flexure, the orientation of the foramen magnum (i.e., differences in the occipital and basicranial regions of the skull) and the doming of the cranial vault. These aspects of skull shape evolution are highly homoplastic across birds and are strikingly similar to those expressed by mammals. Furthermore, as in mammals, larger IRE values (enlarged brains and comparatively shorter basicranial lengths) in birds also often co-occur with ventrally convex cranial bases, a ventral orientation of the foramen magnum, and a shortened facial skeleton. Conversely, lower IRE values, often coincide with relatively enlarged faces, ventrally
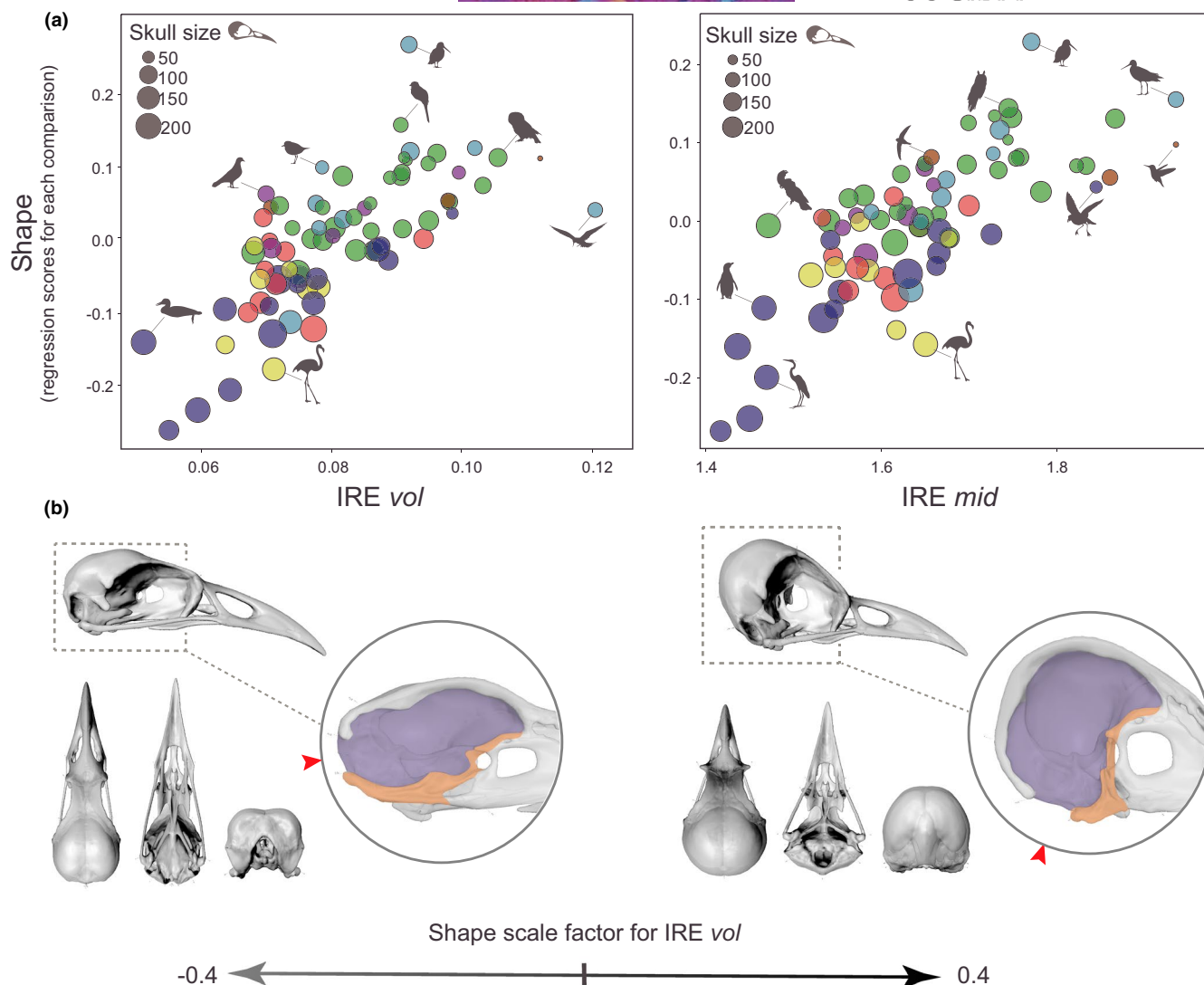
FIGURE 6 PGLS regressions of skull shape (*y*-axes) on IRE *vol* and IRE *mid* (*x*-axes), showing skull size as point size. (a) Scatter-pots. (b) Shape changes predicted by IRE *vol*. Notice, however, that IRE *mid* values are significantly related to a mostly identical shape vector, thus not shown for redundancy. The scale factor for the scores of predicted shape changes was set at ±0.4. The brain's endocast is shown in blue; the reorientation of the foramen magnum is indicated with a red arrow

concave and elongated cranial bases, and a caudally oriented foramen magnum.

These findings suggest that both brain and cranial base size variation, and not just encephalization, are key factors concomitantly underlying avian skull evolution. This is strongly confirmed by our statistical comparisons (Tables S4 and S5) and is further supported by the fact that the traditional IRE ratios were calculated using the length of the cranial base as the denominator (Strait, 1999), by definition. Some non-encephalized birds such as pigeons and small shorebirds share a striking similarity of skull traits with much more encephalized birds like owls, hawks, parrots, and corvids, including a relatively shorter and downwardly oriented face, a ventrally oriented foramen magnum, and a domed cranial vault. This observation suggests that encephalization—which is also highly homoplastic across avian phylogeny—does not on its own account for homoplasy in these aspects of cranial shape. We confirm that here using a statistically

rigorous approach (Tables S3–S5). Our results suggest that the combination of these skull traits is better explained by the interplay between relative brain size and relative cranial base length than by brain size alone (Table S5). This pattern indicates that less encephalized birds attain similar skull shapes to those of more encephalized ones by reducing the length of their cranial bases (i.e., having shorter bases relative to their smaller brains). We note that the same may also be true in mammals and remains overlooked. For example, less encephalized mammalian taxa from most major groups, including marsupials, such as tarsipedids, myrmecobiids and microbiotheres, some bats, some rodents, such as dipodids and some sciurids, and some afrosoricid moles within afrotherians, all exhibit features such as ventrally convex cranial bases and a ventrally oriented foramen magnum (Boddy et al., 2012; Safi et al., 2005; Weisbecker & Goswami, 2010).

Much of the statistical trend that explains the predictions of the SPH in our data set of bird skulls across phylogeny is the scaling
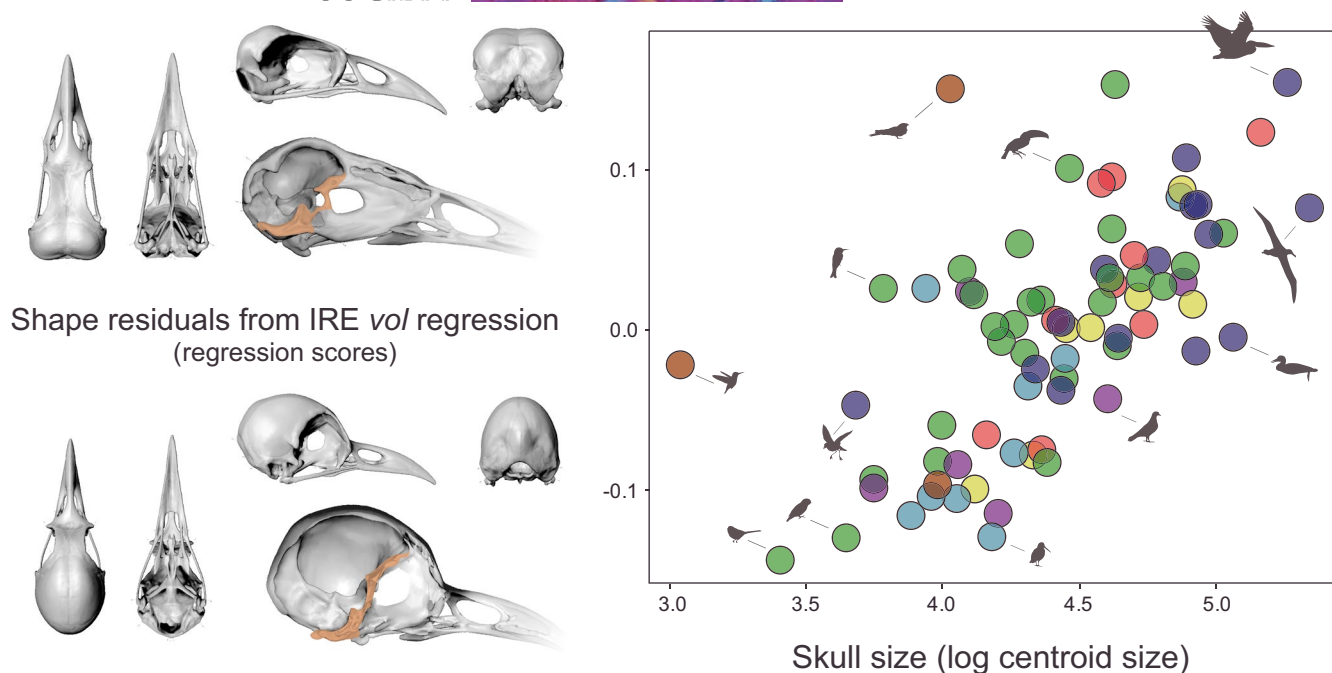
FIGURE 7 Shape residuals from PGLS regression against IRE *vol* plotted against log centroid size of the skull. Notice that the predicted shape changes are devoid of the portion of variance predicted by the IRE *vol* but remain equal to those expressed by evolutionary allometric shape vector (Figure 5)

between brain size relative to the length of the cranial base. Implicit to this finding is the assumption that the interplay between the developmental programs of these two structures are involved in shaping the evolutionary variation of skull morphology, as it has been proposed in mammals (Dubrul & Lasskin, 1961; Jeffery & Spoor, 2002; Strait, 1999). It is well documented that several morphogenetic cues and physical changes during brain development have a cascading effect on the extent and timing of the ossification of cranial vault bones in birds and other reptiles (Fabbri et al., 2017), as well as on the organization and shape of the facial skeleton in chicken, mice, and humans (Boughner et al., 2008; Hallgrímsson et al., 2007; Lieberman et al., 2008; Marcucio et al., 2005, 2015). The involvement of the cranial base in avian skull craniofacial organization entails that the development of the cranial base requires deeper investigation in these organisms. This is a realistic goal because birds are accessible model systems for developmental biology.

Finally, our results underscore the involvement of evolutionary allometry in the observed patterns of skull evolution across crown-group birds. The general pattern of cranial evolutionary allometry that relates the relative sizes of the face and the braincase as a function of body size (now coded with the acronym CREA), has long been found as a pervasive constraint of skull morphological evolution in mammals (Cardini, 2019; Cardini & Polly, 2013; Tamagnini et al., 2017), and of birds (Bright et al., 2016, 2019; Klingemberg & Marugán-Lobón, 2013; Linde-Medina, 2016; Marugán-Lobón & Buscalioni, 2009). According to our findings, the craniofacial expression of the SPH is revealed as another constraint on the skull's evolutionary morphological evolution that seems to be common to these two grand lineages.

Investigating further the pathways linked with the SPH and with the CREA in birds and mammals would be enlightening since the origins of these constraints on skull form possibly have a deep time evolutionary history.

5 | CONCLUSIONS

We explored the features of skull shape evolution in birds that could be explained under the Spatial Packing Hypothesis (SPH), a model morphometrically and experimentally devised to understand skull evolution in mammals. Using whole skull 3D landmark shape data (i.e., incorporating exo and endocranial data), our results showed that the SPH underscores avian craniofacial morphological evolution in a similar way as it does in mammals. However, unlike in the original SPH formalization for mammals, our results show that volumetric encephalization is not the main factor underlying these macroevolutionary patterns in birds. As argued by some authors in mammals, variation in the length of the midline cranial base in birds is also associated with skull evolution. Our results open a prospect in which addressing avian skull variation helps to gain new insight about Amniote skull macroevolution.

AUTHOR CONTRIBUTIONS

JML design the study, JML, SMN, GN, and RB carried out the analyses and wrote the manuscript.

DATA AVAILABILITY STATEMENT

All the authors agree to share the data.

ORCID

Jesús Marugán-Lobón https://orcid.org/0000-0002-3766-8560
Sergio M. Nebreda https://orcid.org/0000-0001-8689-1972
Guillermo Navalón https://orcid.org/0000-0002-2447-1275
Roger B. J. Benson https://orcid.org/0000-0001-8244-6177

REFERENCES

Abzhanov, A., Kuo, W.P., Hartmann, C., Grant, B.R., Grant, P.R. & Tabin, C.J. (2006) The calmodulin pathway and evolution of elongated beak morphology in Darwin's finches. *Nature*, 442, 563–567.

Adams, D.C. & Collyer, M.L. (2018) Phylogenetic ANOVA: Group-clade aggregation, biological challenges, and a refined permutation procedure. *Evolution*, 72(6), 1204–1215.

Adams, D.C. Collyer, M.L. & Kaliontzopoulou, A. (2020) *'Geomorph: Software for geometric morphometric analyses', R package version 3.2.1.* https://cran.r-project.org/package=geomorph

Bastir, M. & Rosas, A. (2009) Mosaic evolution of the basicranium in *Homo* and its relation to modular development. *Evolutionary Biology*, 36, 57–70.

Bastir, M., Rosas, A., Stringer, C., Cuétara, J.M., Kruszynski, R. & Weber, G.W. et al. (2010) Effects of brain and face size on basicranial form in human and primate evolution. *Journal of Human Evolution*, 58, 424–431.

Baumel, J.J. & Witmer, L.M. (1993) Osteologia. In: Baumel, J.J., Evans, H.E. & Van den Berge, J.C. (Eds.) *Handbook of Avian Anatomy: Nomina Anatomica Avium*, 23rd–2 edition. Publications of the Nuttal Ornithological Club, pp. 45–132.

Bhullar, B.-A., Morris, Z.S., Sefton, E.M., Tok, A., Tokita, M., Namkoong, B. et al. (2015) A molecular mechanism for the origin of a key evolutionary innovation, the bird beak and palate, revealed by an integrative approach to major transitions in vertebrate history. *Evolution*, 69(7), 1665–1677.

Bjarnason, A. & Benson, R.B.J. (2021) A 3D geometric morphometric dataset quantifying skeletal variation in birds. *MorphoMuseuM*, 7, e125. https://doi.org/10.18563/journal.m3.125

Boddy, A.M., McGowen, M.R., Sherwood, C.C., Grossman, L.I., Goodman, M. & Wildman, D.E. (2012) Comparative analysis of encephalization in mammals reveals relaxed constraints on anthropoid primate and cetacean brain scaling. *Journal of Evolutionary Biology*, 25, 981–994.

Bookstein, F.L. (1991) *Morphometric tools for landmark data: geometry and biology*. New York: Cambridge University Press.

Bookstein, F.L. & Green, W.D. (1993) 'Thin-plate spline for deformations with specified derivatives'. *Mathematical Methods in Medical Imaging II* (vol. 2035). International Society for Optics and Photonics, pp. 14–28.

Boughner, J.C., Wat, S., Diewert, V.M., Young, N.M., Browder, L.W. & Hallgrímsson, B. (2008) Short-faced mice and developmental interactions between the brain and the face. *Journal of Anatomy*, 213(6), 646–662.

Bright, J.A., Marugán-Lobón, J., Cobb, S.N. & Rayfield, E.J. (2016) The shapes of birds beaks are highly controlled by nondietary factors. *Proceedings of the National Academy of Science of the USA*, 113(19), 5352–5357.

Bright, J.A., Marugán-Lobón, J., Rayfield, E.J. & Cobb, S.N. (2019) The multifactorial nature of beak and skull shape evolution in parrots and cockatoos (Psittaciformes). *BMC Evolutionary Biology*, 19(104).

Brooke, M., Hanley, S. & Laughlin, S.B. (1999) The scaling of eye size with body mass in birds. *Proceedings of the Royal Society B: Biological Sciences*, 266(1417), 405–412.

Cardini, A. (2019) Craniofacial allometry is a rule in evolutionary radiations of placentals. *Evolutionary Biology*, 46, 239–248.

Cardini, A. & Polly, P.D. (2013) Larger mammals have longer faces because of size-related constraints on skull form. *Nature Communications*, 4, 2458.

Collyer, M.L. & Adams, D.C. (2018) RRPP: an R package for fitting linear models to high-dimensional data using residual randomization. *Methods in Ecology and Evolution*, 9(7), 1772–1779.

Collyer, M.L., Sekora, D.J. & Adams, D.C. (2015) A method for analysis of phenotypic change for phenotypes described by high-dimensional data. *Heredity*, 115(4), 357–365.

Couly, G.F., Coltey, P.M. & Le Douarin, N.M. (1993) The triple origin of the skull in higher vertebrates: a study in quail-chick chimeras. *Development*, 117, 409–429.

DuBrul, E.L. & Lasskin, D.M. (1961) 'Preadaptive potentialities of the mammalian skull: an experiment in growth and form'. *American Journal of Anatomy*, 109, 117–132.

Duijm, M.J. (1951) 'On the head posture in birds and its relation features. I-II Proc'. *Koninklijke Nederlandse Akademie Ser. C, Biological and Medical Sciences*, 54, 202–271.

Enlow, D.H. & Hans, M.G. (1996) *Essentials of facial growth*. Philadelphia: W.B. Saunders Company.

Fabbri, M., Mongiardino Koch, N., Pritchard, A.C., Hanson, M., Hoffman, E., Bever, G.S. et al. (2017) The skull roof tracks the brain during the evolution and development of reptiles including birds. *Nature Ecology & Evolution*, 1, 1543–1550.

Felice, R.N., Tobias, J.A., Pigot, A.L. & Goswami, A. (2019) Dietary niche and the evolution of cranial morphology in birds. *Proceedings of the Royal Society B*, 286(1897), 20182677.

Felsenstein, J. (1985) Phylogenies and the comparative method. *American Naturalist*, 125, 1–15.

Friedman, N.R., Miller, E.T., Ball, J.R., Kasuga, H., Remeš, V. & Economo, E.P. (2019) Evolution of a multifunctional trait: shared effects of foraging ecology and thermoregulation on beak morphology, with consequences for song evolution. *Proceedings of the Royal Society B: Biological Science*, 286(1917), 20192474.

Goswami, A., Smaers, J., Soligo, C. & Polly, P. (2014) The macroevolutionary consequences of phenotypic integration: from development to deep time. *Philosophical Transactions of the Royal Society of London B: Biological Sciences*, 369, 20130254.

Gould, S.J. (1975) Allometry in primates, with emphasis on scaling and the evolution of the brain. *Contributions to Primatology*, 5, 244–292.

Gould, S.J. (1977) *Ontogeny and phylogeny*. Cambridge: Harvard University Press.

Hackett, S.J., Kimball, R.T., Reddy, S., Bowie, R.C.K., Braun, E.L., Braun, M.J. et al. (2008) A phylogenomic study of birds reveals their evolutionary history. *Science*, 320(5884), 1763–1768.

Hallgrímsson, B., Lieberman, D.E., Liu, W., Ford-Hutchinson, A.F. & Jirik, F.R. (2007) Epigenetic interactions and the structure of phenotypic variation in the cranium. *Evolution & Development*, 9(1), 76–91.

Herrel, A., Podos, J., Huber, S.K. & Hendry, A.P. (2005) Bite performance and morphology in a population of Darwin's finches: implications for the evolution of beak shape. *Functional Ecology*, 19(1), 43–48.

Hesse, E. (1907) Über der inneren knöcheren Bau des Volgelsechnabels. *Journal of Ornithology*, 55, 185–248.

Hofer, H. (1952) Der gestalwandel des schädels der säugetiere und vögel, mit besonderer berücksichtigung der Knickungstupen und der shädelbasis. *Verhandlungen der Anatomischen Gesellschaft (Jena)*, 50, 102–113.

Iwaniuk, A.N. & Nelson, J.E. (2002) Can endocranial volume be used as an estimate of brain size in birds? *Canadian Journal of Zoology*, 80, 16–23.

Jarvis, E.D., Mirarab, S., Aberer, A.J., Li, B., Houde, P., Li, C. et al. (2014) Whole-genome analyses resolve early branches in the tree of life of modern birds. *Science*, 346, 1320–1331.

Jeffery, N. & Spoor, F. (2002) Ossification and midline shape changes of the human fetal cranial base. *American Journal of Physical Anthropology*, 118(4), 324–340.

Jetz, W., Thomas, G.H., Joy, J.B., Hartmann, K. & Mooers, A.O. (2012) The global diversity of birds in space and time. *Nature*, 491(7424), 444–448.

Klingenberg, C.P. & Marugán-Lobón, J. (2013) Evolutionary covariation in geometric morphometric data: analysing integration, modularity, and allometry in a phylogenetic context. *Systematic Biology*, 62(4), 591–610.

Ksepka, D.T., Balanoff, A.M., Smith, N.A., Bever, G.S., Bhullar, B.-A., Bourdon, E. et al. (2020) Tempo and pattern of avian brain size evolution. *Current Biology*, 30(11), 2026–2036.

Kulemeyer, C., Asbahr, K., Gunz, P., Frahnert, S. & Bairlein, F. (2009) Functional morphology and integration of corvid skulls – a 3D geometric morphometric approach. *Frontiers in Zoology*, 6(1), 2.

Lang, C. (1956) Das Cranium der Ratiten mit besonderer. Beriicksichtigung von Struthio camelus. *Zeitschrift für wissenschaftliche Zoologie*, 159, 165–224.

Lesciotto, K.M. & Richtsmeier, J.T. (2019) Craniofacial skeletal response to encephalization: how do we know what we think we know? *American Journal of Physical Anthropoly*, 168(S67), 27–46.

Lieberman, D.E. (2011) *The evolution of the human head*. Harvard University Press.

Lieberman, D.E., Hallgrímsson, B., Liu, W., Parsons, T.E. & Jamniczky, H.A. (2008) Spatial packing, cranial base angulation, and craniofacial shape variation in the mammalian skull: testing a new model using mice. *Journal of Anatomy*, 212, 720–735.

Lieberman, D.E., Pearson, O.M. & Mowbray, K.M. (2000a) Basicranial influence on overall cranial shape. *Journal of Human Evolution*, 38(2), 291–315.

Lieberman, D.E., Ross, C.R. & Ravosa, M.J. (2000b) The primate cranial base: ontogeny, function and integration. *Yearbook of Physical Anthropology*, 43, 117–169.

Linde-Medina, M. (2016) Testing the cranial evolutionary allometric 'rule' in Galliformes. *Journal of Evolutionary Biology*, 29, 1873–1878.

Maddison, W.P. (1991) Squared-change parsimony reconstruction of ancestral states for continuous-valued characters on a phylogenetic tree. *Systematic Biology*, 40(3), 304–314.

Mallarino, R., Campas, O., Fritz, J.A., Burns, K.J., Weeks, O.G., Brenner, M.P. et al. (2012) Closely related bird species demonstrate flexibility between beak morphology and underlying developmental programs. *Proceedings of the National Academy of Science of the USA*, 109(40), 16222–16227.

Marcucio, R.S., Cordero, D.R., Hu, D. & Helms, J.A. (2005) Molecular interactions coordinating the development of the forebrain and face. *Developmental biology*, 284(1), 48–61.

Marcucio, R.S., Hallgrimsson, B. & Young, N.M. (2015) Facial morphogenesis: physical and molecular interactions between the brain and the face. *Current topics in developmental biology*, 115, 299–320.

Marinelli, W. (1929) Grundriss einer funktionellen Analyse des Tetrapodenschädels. *Palaeobiologica*, 2, 128–140.

Marugán-Lobón, J. & Buscalioni, A.D. (2004) Geometric morphometrics in macroevolution: morphological diversity of the skull in modern avian forms in contrast to some theropod dinosaurs. *Morphometrics*, 157–173.

Marugán-Lobón, J. & Buscalioni, A.D. (2006) Avian skull morphological evolution: exploring exo-and endocranial covariation with two block partial least squares. *Zoology*, 109, 217–230.

Marugán-Lobón, J. & Buscalioni, A.D. (2009) New insight on the anatomy and architecture of the avian neurocranium. *Anatomical record*, 292, 364–370.

McCarthy, R.C. (2001) Anthropoid cranial base architecture and scaling relationships. *Journal of Human Evolution*, 40(1), 41–66.

Monteiro, L.R. (1999) Multivariate regression models and geometric morphometrics: the search for causal factors in the analysis of shape. *Systematic Biology*, 48(1), 192–199.

Navalón, G., Bright, J.A., Marugán-Lobón, J. & Rayfield, E.J. (2019) The evolutionary relationship among beak shape, mechanical advantage, and feeding ecology in modern birds. *Evolution*, 73(3), 422–435.

Navalón, G., Marugán-Lobón, J., Bright, J.A., Cooney, C.R. & Rayfield, E.J. (2020) The consequences of craniofacial integration for the adaptative radiations of Darwin's finches and Hawaiian honeycreepers. *Nature Ecology & Evolution*, 4, 270–278.

Olson, E.C. & Miller, R.L. (1958) *Morphological integration*. Chicago: University of Chicago Press.

Parsons, K.J., Sheets, H.D., Skúlason, S. & Ferguson, M.M. (2011) Phenotypic plasticity, heterochrony and ontogenetic repatterning during juvenile development of divergent Artic charr (*Salvelinus alpinus*). *Journal of Evolutionary Biology*, 24(8), 91640–1652.

Prum, R.O., Berv, J.S., Dornburg, A., Field, D.J., Townsend, J.P., Lemmon, E.M. & Lemmon, A.R. (2015) A comprehensive phylogeny of birds (Aves) using targeted next-generation DNA sequencing. *Nature*, 526, 569–573.

Rambaut, A. & Drummond, A.J. (2014) Tree Annotator v1.8.2. Available from: http://beast.bio.ed.ac.uk/TreeAnnotator

Revell, L.J. (2012) phytools: An R package for phylogenetic comparative biology (and other things). *Methods in Ecology and Evolution*, 3, 217–223.

Rohlf, F.J. (2002) Geometric morphometrics and phylogeny. In: MacLeod, N. & Forey, P.L. (Eds.) *Morphology, shape and phylogeny*. Syst. Ass. Spec. Vol. Ser. 64. London: Taylor and Francis. pp. 175–193.

Rohlf, F.J. & Slice, D.E. (1990) Extensions of the Procrustes method for superimposition of landmarks. *Systematic Zoology*, 39, 40–59.

Ross, C.F., Henneberg, M., Richard, S. & Ravosa, M.J. (2004) Curvilinear and geometric modeling of basicranial flexion in a phylogenetic context: Is it adaptive? Is it constrained? *Journal of Human Evolution*, 46, 185–213.

Ross, C.F. & Ravosa, M.J. (1993) Basicranial flexion, relative brain size, and facial kyphosis in nonhuman primates. *American Journal of Physical Anthropology*, 91, 305–324.

Safi, K., Seid, W.A. & Dechmann, D.K.N. (2005) Bigger is not always better: when brains get smaller. *Biological Letters*, 1, 283–286.

Sayol, F., Downing, P.A., Iwaniuk, A.N., Maspons, J. & Sol, D. (2018) Predictable evolution towards larger brains in birds colonizing oceanic islands. *Nature Communication*, 9, 2820.

Strait, D.S. (1999) The scaling of basicranial flexion and length. *Journal of Human Evolution*, 37, 701–719.

Striedter, G.F. (2005). *Principles of brain evolution*. Sunderland, MA: Sinauer.

Tamagini, D., Meloro, C. & Cardini, A. (2017) Anyone with a long-face? Craniofacial evolutionary allometry (CREA) in a family of short-faced mammals, the felidae. *Evolutionary Biology*, 44, 476–495.

Villmoare, B. (2012) Morphological integration, evolutionary constraints, and extinction: a computer simulation-based study. *Evolutionary Biology*, 40, 76–83.

Weisbecker, V. & Goswami, A. (2010) Brain size, life history, and metabolism at the marsupial/placental dichotomy. *Proceedings of the National Academy of Sciences of USA*, 107(37), 16216–16221.

Wake, D.B., Wake, W.H. & Specht, C.D. (2011) Homoplasy: From detecting pattern to determining process and mechanism of evolution. *Science*, 331(6020), 1032–1035.

Werner, C.F. (1962) Allometrische Grossenunterschiede und die Wechselbeziehung der Organe (Untersuchungen am Kopf der Vögel). *Acta anatomica*, 50, 135–157.

Young, N.M., Hu, D., Lainoff, A.J., Smith, F.J., Diaz, R., Tucker, A.S. et al. (2014) Embryonic bauplans and the developmental origins of facial diversity and constraint. *Development*, 141, 1059–1063.

Zusi, R.L. (1993) Patterns of diversity in the avian skull. *The skull*, 2, 391–437.

SUPPORTING INFORMATION

Additional supporting information may be found in the online version of the article at the publisher's website.

How to cite this article: Marugán-Lobón, J., Nebreda, S.M., Navalón, G. & Benson, R.B.J. (2022) Beyond the beak: Brain size and allometry in avian craniofacial evolution. *Journal of Anatomy*, 240, 197–209. https://doi.org/10.1111/joa.13555